Colloid Polym Sci 275:91–95 (1997)

SHORT COMMUNICATION

H.-J. Schwenn
M. Wark
G. Schulz-Ekloff
H. Wiggers
U. Simon

Electrical and optical properties of zeolite Y supported SnO_2 nanoparticles

Received: 18 June 1996
Accepted: 29 August 1996

H.-J. Schwenn · M. Wark · G. Schulz-Ekloff
Universität Bremen
Institut für Angewandte und
Physikalische Chemie
Leobener Straße NW 2
28359 Bremen

H. Wiggers · Dr. U. Simon (✉)
Universität Essen
Institut für Anorganische Chemie
Schützenbahn 70
45127 Essen

Abstract Meso- and nanoporous solids used as supports for highly dispersed metal or semiconductor nanoparticles represent a promising class of materials for potential nanoscale devices. The electrical and optical properties of zeolite Y supported SnO_2 nanoparticles were studied by use of impedance and UV diffuse reflectance spectroscopy. When subjected to reductive and oxidative atmospheres the samples reveal sensitive changes in their properties which are different to that of bulk SnO_2.

Key words Semiconductor – nanoparticles – zeolite – sensor – UV-spectroscopy – impedance spectroscopy

The development of nanoscaled host/guest compounds has offered a rapidly growing and explorative field of research in the last few years. In most cases oxide framework or layered structures like nanoporous zeolite molecular sieves and related structures, like AlPOs or SAPOs, mesoporous MCM materials and related metal oxide phases as well as pillared clays are used as supports for highly dispersed guest compounds. Metal or semiconductor nanoparticles are of immense interest as guests due to quantum size effects which determine the physical properties of matter in the size regime of a few nanometers. In any case these materials represent a promising variety of low dimensional compounds for potential nanoscale devices [1, 2].

In this paper we report about the investigation of electrical and optical properties of SnO_2 nanoparticles which are dispersed in a zeolite Y matrix. Since bulk SnO_2 has a technical application as gas sensor material [3], the electrical and optical properties of zeolite supported SnO_2 nanoparticles in contact with different gas atmospheres are examined to determine if i) the molecular sieve effect of the host and ii) the tuning of the semiconductor dispersion could result in improved sensor properties.

To determine the electrical properties of the dispersed SnO_2 nanoparticles and to separate them from those of the zeolite matrix which is known to be an ionic conductor [4–9], impedance spectroscopy (IS) should be a suitable method. The optical properties of semiconductor nanoparticles, i.e., changes in the width of the band gap or the formation of localized states for electrons, can be obtained from absorption properties studied by UV diffuse reflectance spectroscopy (UV-DRS).

The chemical procedure of incorporation of SnO_2 nanoparticles has already been reported for zeolites of the mordenite and the faujasite type [10–12]. For the following investigations SnO_2 nanoparticles encapsulated in synthetic NaY with an Si/Al ratio of 2.87 were prepared by conventional ion exchange from a $SnCl_2$ solution as described elsewhere [11, 12]. The Sn content in the samples studied was determined, after dissolving parts of the samples in HF, by atomic absorption spectroscopy and ranged from 1–11 wt %. After calcination, which also led to a slight loss of lattice aluminum up to a Si/Al ratio of 3.19,

the size and the dispersion of the SnO_2 nanoparticles determined by transmission electron microscopy (TEM; Phillips EM 420) were sound to depend on the Sn loading. High loadings (> 4 wt-% Sn) promote the formation of a broad range of particle size distribution from 2 to 20 nm (Fig. 1).

Diffuse reflectance UV spectra were recorded in situ at 293 K with a Varian Cary 4 spectrometer in a specially designed gas cell. The pressed samples were at least 2 mm thick and can therefore be regarded as infinitly thick, as required by the Kubelka–Munk theory. After dehydration of the samples at 673 K, spectra were recorded under vacuum and under O_2, H_2 and CO (pressure: 10^5 Pa) at 293 K. Since at wavelengths below 250 nm the reflectance is rather low and scattering effects cannot be fully ignored, all samples were referred to a reflecting standard (LOT 75%) and reproduced several times.

The UV spectra of these samples, however, reveal blue-shifts of the absorption edges of about 20–30 nm compared to the edge of bulk SnO_2. Applying the "effective mass approximation", which was established by Brus [13], onto these values, particle diameters of 2–4 nm were estimated. We assume that the apparently larger particles observed on the TEM micrographs (see Fig. 1) represent agglomerates of several smaller nanoparticles (cluster assemblies). The presence of agglomerates might furthermore be responsible for the strong tailing in the UV spectra.

Although the band edge position is not markely changed by the surrounding gas atmospheres, the maximum of absorption is significantly decreased and red-shifted by H_2 and CO and enhanced and blue-shifted by O_2, respectively (Fig. 2). These changes probably result from the excitation of electrons into localized states below the conduction band or into surface states [14], both being formed in reductive and eleminated in oxidative atmospheres. For bulk SnO_2 physically mixed with NaY (inset of Fig. 2) an extinction with a sharp absorption edge typical for bulk semiconductors was found. The extinction depends less on the surrounding gas atmosphere, since the electronic structure of the band gap was dominated by the huge number of non-affected states in the bulk.

In the presence of CO a partial formation of tin carbonate species, as they were found in FT-IR measurements under comparable conditions [15], may also influence the absorption spectra.

For impedance measurements pressed pellets with a diameter of 5 mm and an average thickness of 0.3–0.4 mm were contacted mechanically by polished platinum electrodes and inserted into a high temperature measuring cell similar to that described by Schön et al. [16]. All samples have been dehydrated, by heating at 673 K for 48 h under an Ar pressure of 0.1 Pa. The spectra were taken in the frequency range from 10 Hz to 10^7 Hz (HP 4192 A Impedance Analyzer) and in a temperature range from 293 to

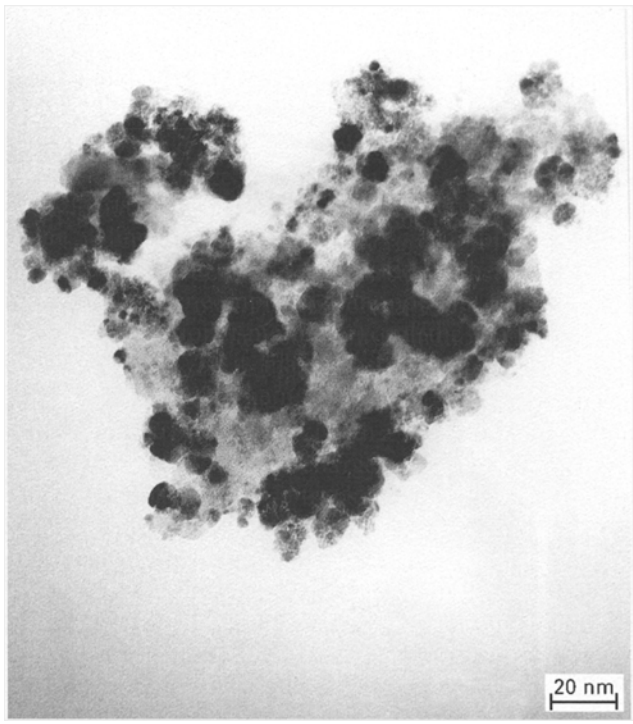

Fig. 1 Electron transmission micrograph of zeolite Y supported SnO_2 nanoparticles (magnification 1:750 000, inserted bar indicates 20 nm)

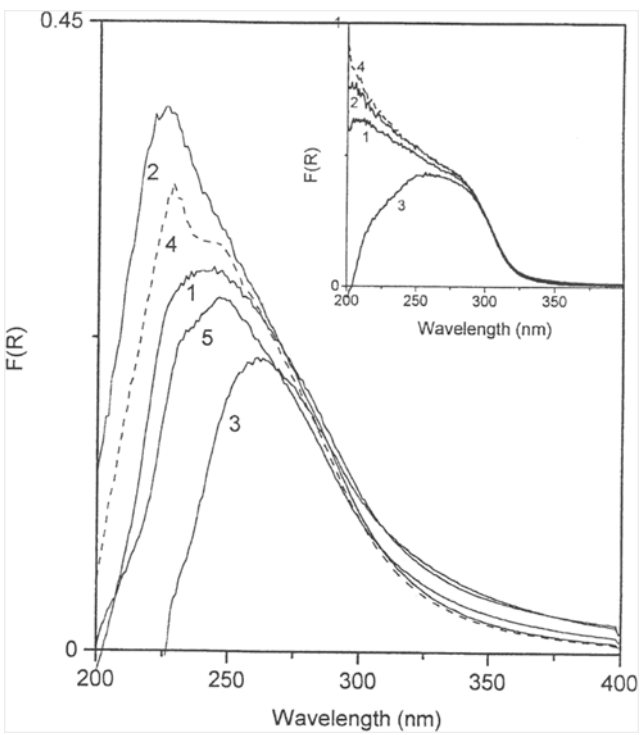

Fig. 2 UV absorption spectra of NaY/SnO_2 (11 wt % Sn) and, as inset, bulk SnO_2, physically mixed with NaY, in 1) vacuum, 2) O_2, 3) CO, 4) O_2 after CO 5) H_2

673 K at intervals of 10 K under vacuum or the corresponding gas atmosphere at 0.1 Pa. Dc-conductivity was probed up to 1 GΩ.

The measurements on dehydrated NaY show a semicircle with a low frequency tail in the complex impedance plane (Fig. 3). The diameter of the semicircle decreases with increasing temperature indicating the thermal activation of conductivity.

In general the relaxation mode corresponding to the semicircle resembles the behavior of various types of zeolites like zeolite A [4], faujasite [5–7], analcite [8] and related structures [9], conductivity of which has been studied in earlier works. As described there, it is caused by the motion of the cations (Na^+) as a sequence of cation hopping between the well defined cation sites in the cages (dipolar relaxation) and along the channels of the negatively charged zeolite lattice to give a long-range charge transport.

The temperature dependence of conductivity can be described by the Arrhenius relation and the corresponding activation enthalpy E_A is $78 \pm 3\ kJmol^{-1}$ for the Na^+ form. The values of the specific conductivity and the E_A are in good agreement with those reported earlier for the faujasite type [6]. The low-frequency part of the impedance plot is dominated by the sample/electrode interface polarization expressed by the low-frequency tail. This is typical for various ionic conductors when blocking electrodes are applied. It can be interpreted in terms of the infinite case of the Warburg impedance by the absence of a dc-conductivity [17].

The NaY samples with incorporated SnO_2 nanoparticles reveal an additional relaxation mode which appears at lower frequencies than the bulk relaxation (Fig. 4). According to ref. [10] we ascribe the appearence of the second relaxation mode to the presence of SnO_2 nanoparticles.

At high temperature ($T > 555$ K) the thermal activation of the total conductivity is approx. equal for the NaY and the NaY/SnO_2. In this temperature range ionic conductivity dominates. The conductivity of the samples containing SnO_2 is somewhat lower than those of the Na^+ form, since the exchange of Na^+ by Sn^{2+} leads to a decreased number of mobile charge carriers. At lower temperature the activation enthalpy of NaY/SnO_2 is $5\ kJmol^{-1}$ (taken at the highest content of SnO_2).

By changing the surrounding gas atmosphere we observed that the impedance of pure faujasite is not influenced by H_2 and O_2. Earlier investigations on the absorption of N_2 and O_2 in faujasite indicate that at low temperature (197 K) the conductivity increases due to a weak interaction between the Na^+ ions and the absorbed gas molecules. As can be inferred from ref. [17], this effect may be neglected at temperatures above 273 K. This seems to be conclusive with the results we obtained in the high temperature range studied here. In contrast to the pure faujasite the conductivity of the NaY/SnO_2 samples is

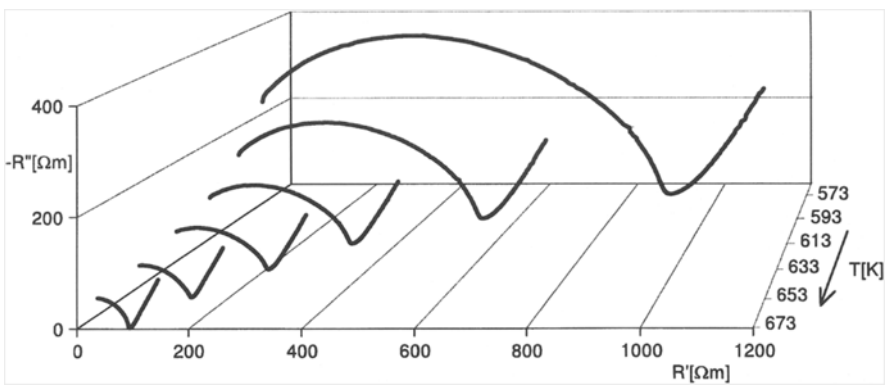

Fig. 3 Argand diagram (plot of the scaled imaginary part of the impedance R'' against the scaled real part of the impedance R' in the complex plane) of dehydrated zeolite NaY for different temperatures between 573 to 673 K. From the low frequency minimum the specific conductivity can be obtained

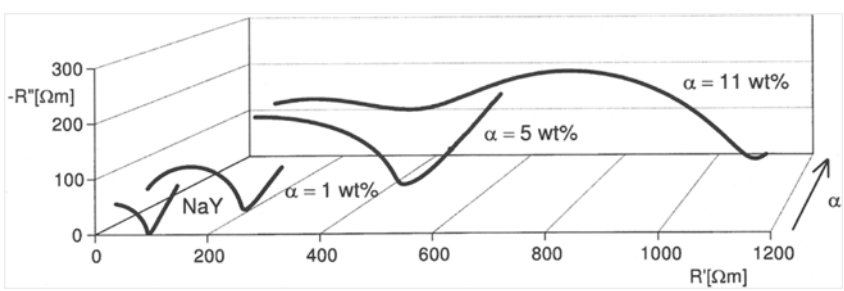

Fig. 4 Argand diagram of zeolite NaY and NaY supported SnO_2 nanoparticles (α = 1, 5 and 11 wt.-% Sn, resp.) at 673 K

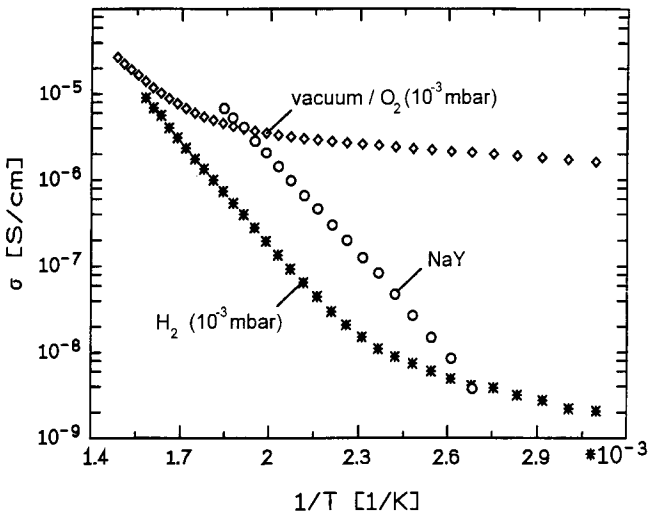

Fig. 5 Arrhenius plot of NaY in vacuum and NaY supported SnO_2 nanoparticles (11 wt.-% Sn) in vacuum, O_2 and H_2, resp.

extremely affected by the surrounding gas atmosphere. While Ar, vacuum and O_2 lead to the same temperature dependent conductivity, H_2 causes a strong decrease in conductivity. This effect is more significant at lower temperature (down to 320 K) and higher Sn content.

This behavior is surprising since it is opposite to that of bulk SnO_2, where reductive agents increase the dc-conductivity, indicating a different mechanism of conductivity. In bulk SnO_2 the charge carrier density depends on the purity and stoichiometry. Therefore reductive gases like H_2 and CO increase, while O_2 decreases the dc-conductivity as well as the extinction of interband absorption.

To describe our experimental findings a new model for the underlying microscopic processes has to be proposed: NaY/SnO_2 samples exhibit no dc-conductivity since the volume fraction of SnO_2 within the zeolilte matrix is below the critical concentration to reach the percolation threshold, i.e., to enable an electronic long-range charge transport. The appearance of a second relaxation mode indicates that a local charge transport takes place. The low activation enthalpy excludes an ionic process of mobile tin or oxygen ions. A local charge transport may result from hopping or tunneling of charges between neighbouring nanoparticles within the assemblies seen on TEM micrographs (Fig. 1). These assemblies behave like larger particles and form conduction paths with low conductivity, in which the nanoparticles are separated by the resistance of hopping or tunneling barriers. At the same time the spatial distance between the assemblies is too large to enable a long range charge transport to give a dc-conductivity.

The nature of this relaxation process is not yet understood in detail. Basing on the consideration described above, we assume that the decrease of conductivity in H_2 atmosphere may result from a decrease of the concentration of stoichiometric SnO_2 nanoparticles with a preserved band structure per volume unit and per cluster assembly. The resulting particles mainly consist of non stoichiometric SnO_x ($x < 2$) with a huge number of defects and localized states where charge carriers may be trapped, reducing the local charge transport.

The decrease in the number of stoichiometric SnO_2 nanoparticles under reductive atmospheres is confirmed by the decrease of the integral absorption and the red-shift of the maximum in the UV absorption spectra (Fig. 2) in agreement with our results that the red-shift derives from the formation of defect states. Consequently, the maximum of the absorption shifts to higher energies if the defects were "healed" by the treatment with oxygen. The as-prepared sample, where electronic defects already exist, exhibits a surplus of tin ions for charge compensation of the polyanionic zeolite framework. The resulting strong interaction with the host is indicated by an increase in the full width of half maximum (FWHM) of the SnO_2 signal in ^{119}Sn MAS NMR spectra [12].

In conclusion, the strong changes of the optical extinction and the impedance spectra upon switching between oxidative and reductive gas environment provide a basis for application of zeolite supported semiconductor nanoparticles as sensors. Our work will be expanded to other systems (e.g. TiO_x/NaY) for which a similar behavior should be expected. We will concentrate on the preparation of dispersions of smaller particles with narrow particle size distribution to obtain more information about the nature of the conductivity mechanism.

Acknowledgment Financial support by the Bundesminister für Forschung und Technologie (BMFT under contract Nrs. 03 C 2006 9 and 03 C 2005 8) is greatfully acknowledged.

References

1. Ozin GA (1992) Adv Mater 4:612 and references therein
2. Schön G, Simon U (1995) Colloid Polym Sci 273:101 and 273:202
3. Göpel W, Hesse J, Zemel JN (eds) (1989) In: Sensors. VCH, Weinheim, and references therein
4. Simon U, Möhrke C, Schön G (1995) Chem Ing Tech 67:583
5. Freeman DC, Stamires DN (1961) J Chem Phys 35:799
6. Schoonheydt RA, Uytterhoeven JB (1969) Clay Minerals 8:71
7. Stamires DC (1973) Clays and Clay Minerals 21:379
8. Beattie IR (1954) Trans Faraday Soc 50:581
9. Oguschi T, Kawanabe Y (1994) Zeolites 4:365

10. Knudsen N, Krogh Andersen E, Krogh Andersen IG, Skou E (1988) Solid State Ionics 28–30:627 and Krogh Andersen IG, Krogh Andersen E, Knudsen N, Skou E (1991) Solid State Ionics 46:89
11. Wark M, Schwenn HJ, Schulz-Ekloff G, Jaeger NI (1992) Ber Bunsenges Phys Chem 96:1727
12. Wark M, Schwenn HJ, Warnken M, Jaeger NI, Boddenberg B (1995) Stud Surf Sci Catal 97:205
13. Brus LE (1986) J Phys Chem 90:2555
14. Weller H (1993) Angew Chem 105:43
15. Schwenn HJ, Wark M, unpublished results
16. Lortz W, Osswald W, Kelemen G, Schön G (1989) J Phys E Sci Instrum 22:293
17. MacDonald JR (1987) Impedance Spectroscopy, Wiley & Sons, New York
18. Breck DW (1974) Zeolite Molecular Sieve, Wiley & Sons, New York